

Deconvolving seismic signals with a SPICE model of the seismometer.

Giovanni Romeo

Istituto Nazionale di Geofisica e Vulcanologia

Abstract

Every transducer needs some deconvolution operation to return the original signal. In the seismometer's case this is usually done by using the pole-zero instrument models. This method assumes that the seismometer can be described by a linear model that can be schematized by a ratio of polynomials of the Laplace variable s . This paper shows a deconvolution method that uses the mechanic-electric model of a transducer. This more accurate modelling of a seismometer gives a better description of a transducer since it can also take into account non-linear behavior which cannot be included in pole-zero models. Examples of deconvolution of both linear and non-linear transfer functions are shown, and some considerations about friction damping and the electromechanical analogies used to perform the simulations are included in the appendix.

Note: convolution and deconvolution are mathematically defined as linear operations. Therefore a non-linear deconvolution is a non sense. In the article, the locution 'non linear deconvolution' should be intended as non-linear reconstruction.

Keywords:

Seismometer, pSPICE model, deconvolution, Coulomb damping.

1. Inverse transfer function

Let's consider the functional block in fig. 1. It operates on the input signal, producing an output signal. When $F(s)$ represents a transducer, input and output will not have the same physical dimensions; in the seismometer's case the input will be something related to the ground movement, and the output will be a voltage (something easily handled by an acquisition system).

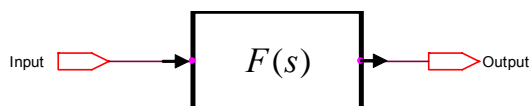


Fig 1. A transducer can be represented by a functional block that produces an output signal operating on an input stimulus.

Functional blocks can be easily modeled by simulation programs developed for electronics, and they are especially useful for the treatment of non-linear cases.
In the schematic of fig. 2 we have re-arranged the functional block of fig.1

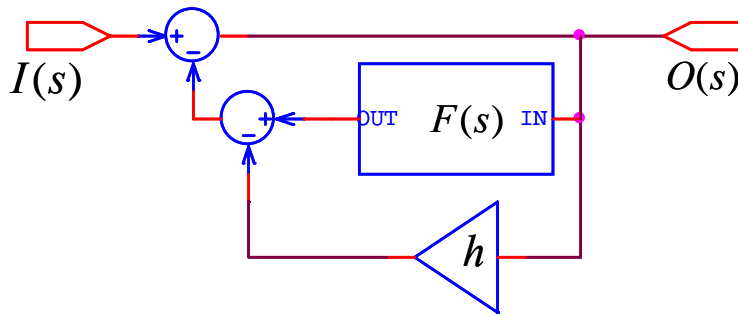


Fig.2 The transfer function of the schematic in the picture approximates the inverse of $F(s)$ (see text)

From the schematic fig.2 we obtain:

$$O(s) = I(s) - F(s) \cdot O(s) + h \cdot O(s) \quad (1)$$

$$\frac{O(s)}{I(s)} = \frac{1}{F(s) + 1 - h} \quad (2)$$

If $h=1$ $O(s)/I(s)=1/F(s)$, so the circuit of fig 2 is the inverse function of $F(s)$ and may be used to calculate the original signal transduced by a sensor with transfer function $F(s)$.

A typical seismometer transfer function is shown in equation (3) (k is a normalization coefficient) and has the Bode graphical representation shown in fig. 3.

$$F(s) = \frac{s}{(s+a)(s+b)} k \quad (3)$$

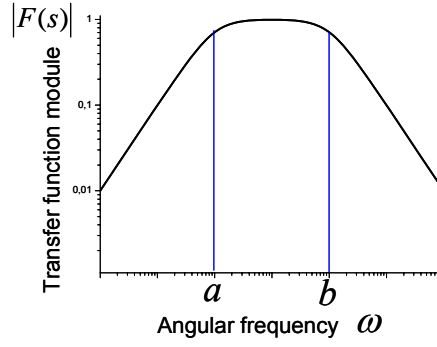


Fig.3 Typical seismometer's frequency response (Bode representation of equation (3)). log-log

Equation (4) represents the inverse of equation (3) obtained combining equation (3) and equation (2). The Bode representation of (4), parameterized for different values of h , is shown in fig. 4.

$$G(s) = \frac{1}{\frac{sk}{(s+a)(s+b)} + 1 - h} \quad (4)$$

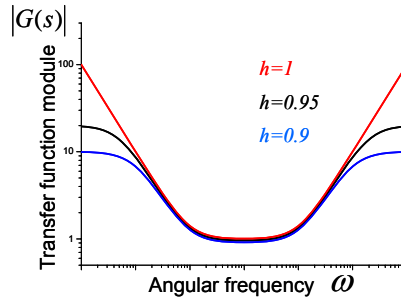


Fig.4 the Bode representation of the (4) parametrized for 3 values of h

For values of h approaching 1, $G(s)$ approximates $1 / F(s)$ increasingly well. When h decreases, only the central part of the function is approximated. The Bode diagram of the product $F(s) G(s)$ is shown in fig. 5

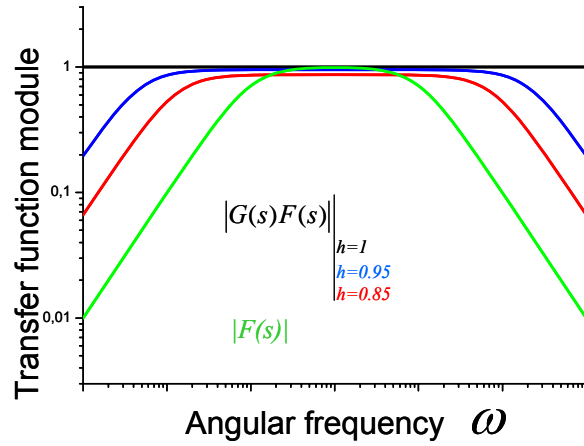


Fig. 5. The Bode diagram of $F(s)G(s)$. $G(s)$ has been parameterized with different values of h . The original diagram of $F(s)$ is drawn in green.

Fig 5 shows 3 deconvolution curves for $h=1$ (black), $h=0.95$ (blue) and $h=0.85$ (red). If we compare the original function with the deconvoluted signal we see that the deconvolution extends the bandwidth of the sensor (which is what we want) around the central area, and reduces the tails. This behavior has a practical utility. Although it is formally possible to correct any function by applying its inverse function, this method cannot be used in practice. When the response of the transducer attenuates the signal (this happens at the tails of the transfer function) down to the noise level (electrical or sampling noise), the exact deconvolution ($h=1$) is not possible: at the tails, where the inverse of the function of the transducer has very high gains, the signal/noise ratio of the transducer is very low and the deconvolution accentuates the noise. On the other hand, the approximate deconvolution ($h<1$) limits the amplification at the tails, and this effect can be tuned by changing the h value.

2. A practical example: the S13 geophone deconvolution.

The S13 seismometer model [Romeo, 2012] is shown in fig.6. pSPICE has been chosen because it is well known and allows easy modelling of electric, and mechanic, components. For mechanic parts we may either use Laplace blocks or some electrical-mechanic equivalent. In case of arbitrary waveform stimulus, the electrical-mechanic equivalent gives better results.

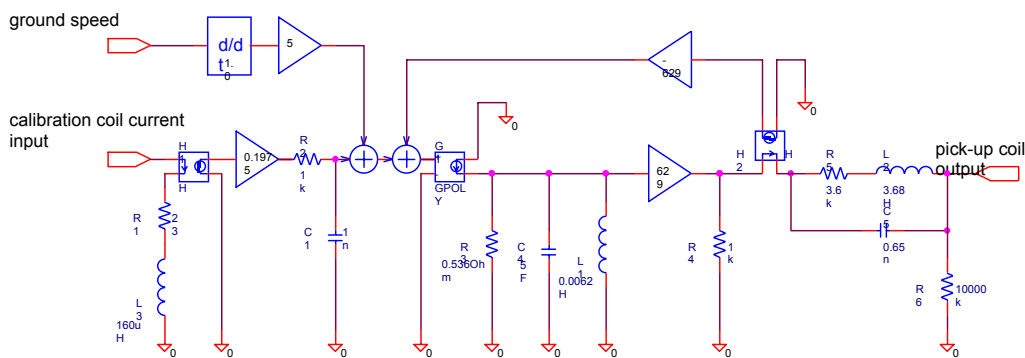
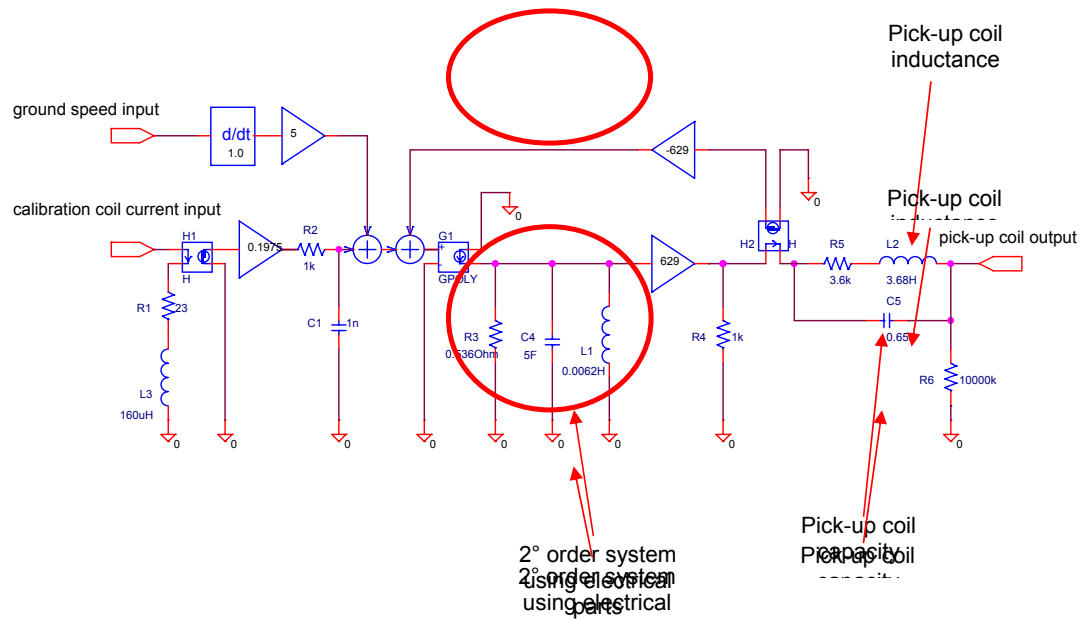


Fig.6 this is the model of the Teledyne Geodic S13 seismometer [Romeo, 2012]. Here we assume that the seismometer is stimulated with an acceleration signal, in this way the derivative block connected to the ground speed input can be ignored. R6, which is assigned an extremely high value, has no physical meaning, but is used to formally close the output link.

To check the performance of the circuit in fig.2 we used the seismometer model both inside and outside the deconvolution block, as described in fig. 7.

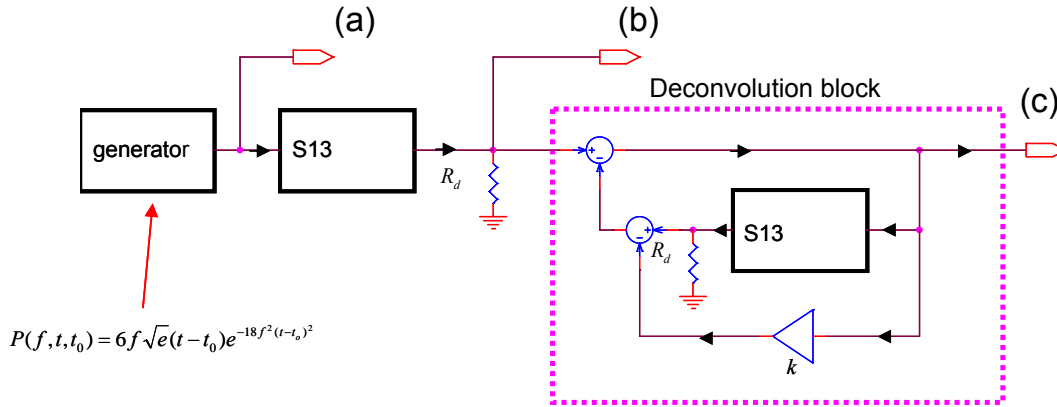
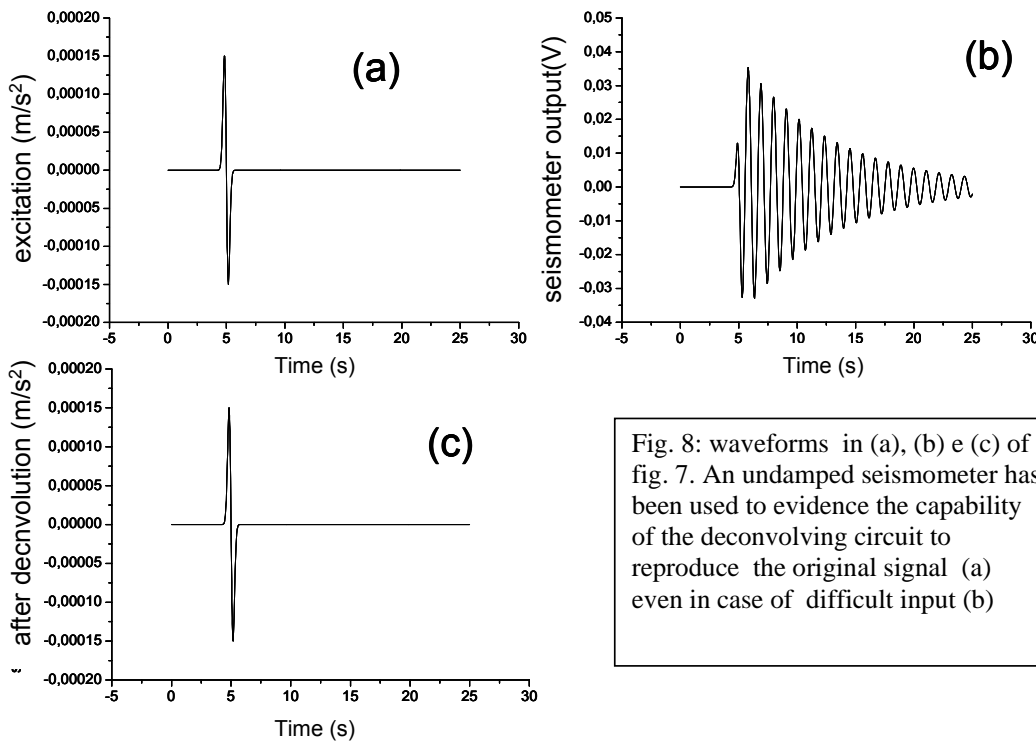


Fig 7. Model used to verify the deconvolution recipe of fig. 2. R_d is the damping resistor. The stimulus ($P(f, t, t_0)$), a Gaussian function derivative, offers a single-waveform, continuous, 0-mean, easily tunable, single oscillation.

Fig. 8 shows the waveforms corresponding to points (a), (b) and (c) of fig.7.



Commento [Stephen 1]: Scale temporali: in Fig. 8 a e b cambiare tempo in time. In 8 c aggiungere (s)

Fig. 8: waveforms in (a), (b) e (c) of fig. 7. An undamped seismometer has been used to evidence the capability of the deconvolving circuit to reproduce the original signal (a) even in case of difficult input (b)

The miracle in fig 8 is only mathematical. The real world is much less tolerant. In the critical case of an undamped seismometer even a very small difference between the seismometer and the model is enough to spoil the output. Fig 9 (a) represents the deconvolution of the signal represented in fig. 8 (a) when a mismatched model in the deconvolution block is used (the mass has been augmented from 5 to 5.5 kg). This output error can be decreased just by adding a 4KOhm damping resistor (roughly the critical damping). In Figure 9 (b), the red trace represents the stimulus, the blue and the green traces the deconvolution with the model with the mass increased respectively to 5.5 and 8 kg.

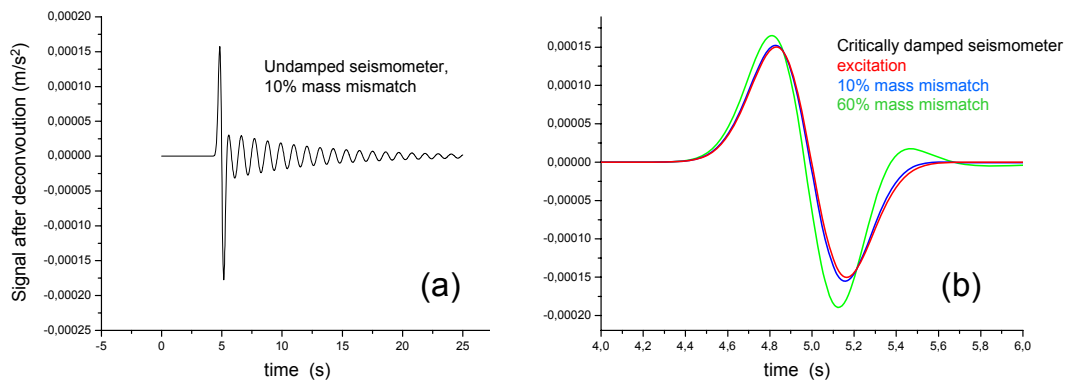


Fig 9. Deconvolution of the stimulus of fig 7(a) with some model mismatch. (a) represents the output of undamped models with 0.5 Kg (10%) mass mismatch between the models. (b) shows the stimulus signal (red) and two outputs with 0.5 kg mismatch (blue) and 3 Kg mismatch (green).

3. Non linear deconvolution

The described method offers good results in the deconvolution of nonlinear models (see A1). Fortunately we do not need this recipe to deconvolve modern seismometers, since a pole-zero model completely describes the instrument. On the other hand, this method for non-linear deconvolution can be used to reconstruct the signals of old seismometers, which directly record on paper, and in which part (or all) of the damping was induced by the friction of the mechanics and of the tip writer. As the sliding friction depends only on the velocity sign (neglecting the static friction), the equation of a traditional driven oscillator,

$$m\ddot{y} + c\dot{y} + gy = gax$$

becomes:

Commento [Stephen 2]: Sc
hemino meccanico ?

$$m\ddot{y} + \left(c + \frac{d}{|\dot{y}|}\right)\dot{y} + gy = gax \quad (5)$$

Equation (5) shows two damping contributions. The first term, c , represents viscous damping, the second term, $\frac{d}{|\dot{y}|}$, represents sliding friction (Coulomb damping).

The impulse response of the system described by equation (5) (we defined $c=0$ to keep only the effect of the sliding friction) has an atypical shape, with a linear decrease of the envelope of the oscillations (Fig. 8). A simple explication of such atypical decay is done in A.2. Fig. 10 was obtained using the undamped model of the geophone s13 (fig 6), with some modification in the circled part (A.3).

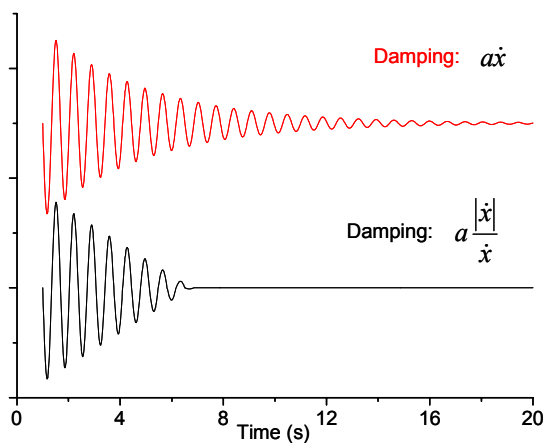


Fig. 10 The red trace shows the typical exponential decay of an harmonic oscillator (1 sec, damping = 0.034) with the velocity-dependent damping term. The black trace shows the effect of a damping. Damping depends only on the sign of the speed and produces a linear decay.

Fig 11 shows the result of the deconvolution process when the sliding friction induced damping is acting. The stimulus is the same one we used in fig. 8. Note the linear decay of the seismometer output (b) and the perfect reproduction of the stimulus at the output of the deconvolving block (c). Fig. 12 shows an ancient recording (1916) from the Porto d'Ischia observatory. A pulse response shows a nearly perfect triangular-shaped decay caused by the Coulomb damping. Such kind of recordings allow us to evaluate the parameters of ancient seismometers and to build models to deconvolve their seismograms.

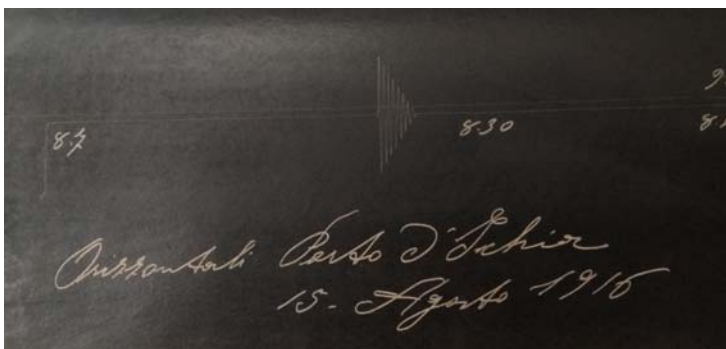
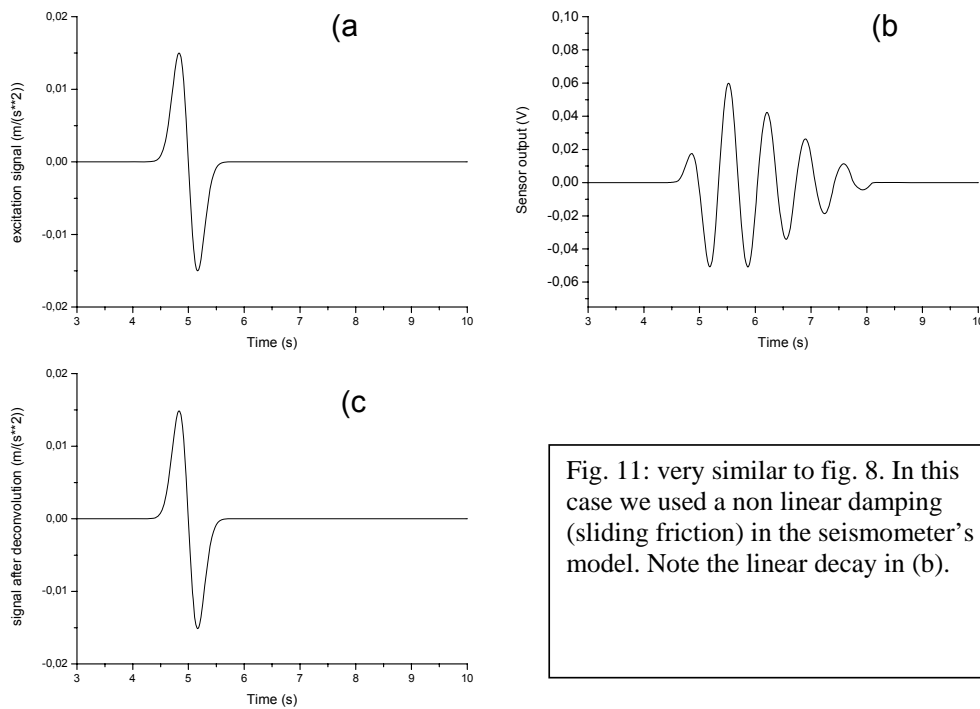


Fig. 12. A calibration pulse on the ancient Grablovitz seismometer in Porto d'Ischia observatory (1916). The pulse response shows a perfect triangular decaying shape caused by the writing tip on the paper.

Acknowledgements

I thank Graziano Ferrari, for the interest demonstrated in the deconvolution method and for the access to the SISMOS archive. I thank also my colleague Stephen Monna for reading the manuscript and for giving some precious suggestion.

Appendices.

A-1

The use of the principle shown in fig. 1 to de-convolve a non linear transfer function may be justified in the following way.

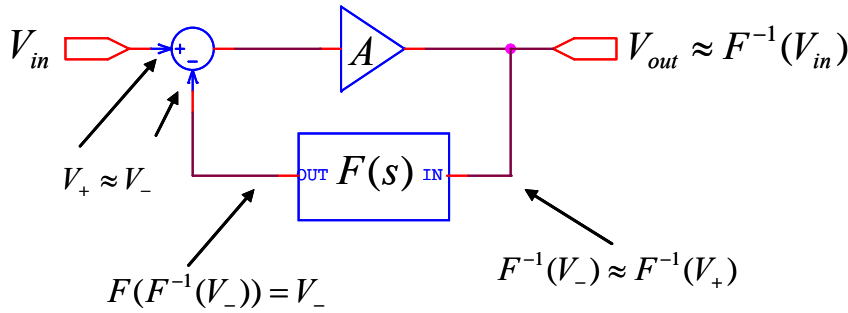


Fig. 12 If the gain of the amplifier $A \gg 1$, and assuming stability, the circuit acts as nullor, i.e. it tries to make V_- to follow V_+ regardless of the behavior of $F(s)$ (even when it is non-linear), thus forcing $V_- \approx V_+$. This is accomplished also by the circuit in fig. 2 as it is equivalent to the one in fig. A.1 if $A = 1/(1-h)$

Fig. A1 shows a configuration engineers call ‘nullor’. Assuming the stability of the circuit, this configuration causes the voltage between the inputs V_+ and V_- to be zero, regardless of the behavior of $F(s)$ even non linearities. Block $F(s)$ will output V_- if we feed it the signal $F^{-1}(V_-)$; therefore the circuit of fig. A.1 applies the F^{-1} operator to the V_{in} signal. Since circuit in fig 12 is equivalent to the circuit in fig 2 if we assume $A = 1/(1-h)$ the circuit of fig. 2 can also handle non linear transfer functions.

A.2. Linear decay in case of sliding friction.

If we neglect viscous friction and the external force in equation (5),

we obtain:

$$m \ddot{y} + \frac{\dot{y}}{\square} r + gy = 0 \quad (6)$$

we may also neglect the static friction. This assumption is especially valid in the seismometer's case, where we assume that the friction is concentrated mostly between the writing device and the paper, and the paper never stops moving so the system never enters the static friction condition. Equation (A.2.1) may be split in two equations, one for each direction of motion,

$$m \dot{y} + \dot{y} r + gy = 0 \quad (7)$$

$$m \dot{y} - \dot{y} r + gy = 0$$

The peculiarity we observe in sliding friction induced damping is the shape of the envelope, linear instead of exponential. This can be justified without a complete solution of the (A.2.2).

Let's assume that the oscillation starts at rest from a point y_0 and energy E_0 , and reaches a point y_1 (just before changing its direction of motion), with energy E_1 .

At the starting point y_0 the energy is completely concentrated in the spring, when $y=0$ the energy is completely converted into the kinetic energy of the mass, and, at the end of the oscillation, energy is again concentrated in the spring, just before the change of motion direction (fig.A.2.1). The potential energy is a function of the spring length:

$$E_{spring}(y) = \int_0^y g x dx = \frac{1}{2} g y^2$$

And the energy dissipated by friction during the travel depends only of the travel length:

$$E_{loss}(y) = r y$$

The difference between the energies from the start, y_0 , to the first relative minimum, y_1 , must be equal to the energy dissipated by friction during the travel from y_0 to y_1 .

$$E_0 - E_1 = \frac{1}{2} g (y_0^2 - y_1^2) = r (y_0 - y_1)$$

This energy should be the energy lost in friction.
With some simple math:

$$(y_0 - y_1) = \frac{2r}{g}$$

So the amplitude loss for every semi-oscillation is constant and depends only of the friction coefficient and the spring constant.

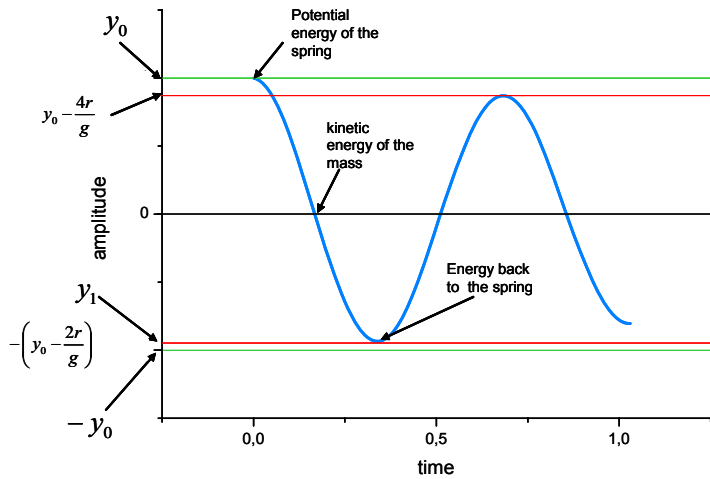


Fig A.2.1. Coulomb decaying plot. Every oscillation the amplitude decreases of $4r/g$, where r is the damping force and g the spring coefficient.

A.3 mechanical simulation in pSPICE

Mechanical assemblies and electrical circuits share the same equations with some redefinition of symbols, and this allows the use of electrical simulators to model mechanical devices, such as a seismometer.

An RLC parallel circuit has the same mathematical representation of a damped mechanic oscillator, if we associate the capacitor to the mass, the inductor to the coil and the resistor to the damper. The voltage across the parallel oscillator is associated to the speed; the current through each component represents the force on its associated mechanical component.

Velocity and Coulomb damped oscillators in their electrical form are represented in fig. A.3.2.

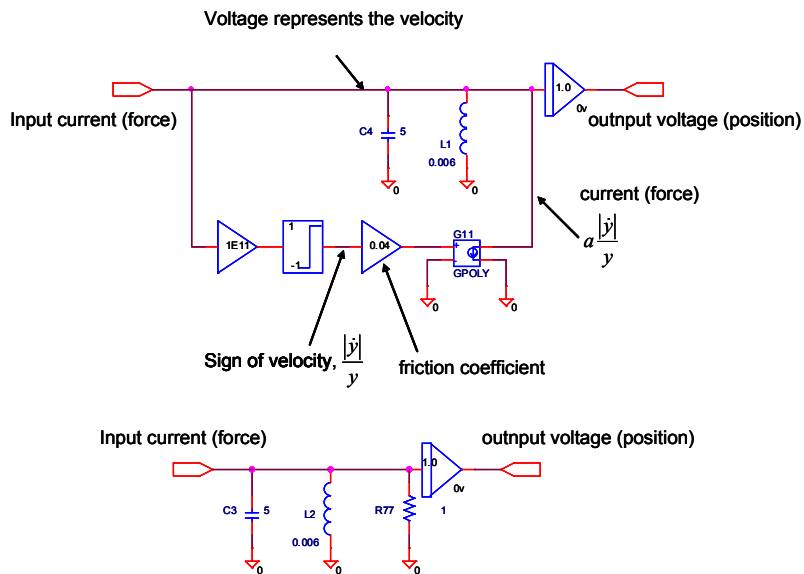


Fig A.3.2 Upper image shows the equivalent circuit of a Coulomb damped oscillator; lower image shows the equivalent circuit of a velocity damped oscillator.

The two oscillators are identical except for the resistor. To simulate the Coulomb damper, the voltage (which corresponds to velocity) has been amplified and clipped to ± 1 and has been used to change the sign to the friction coefficient. The velocity damper uses a simple resistor.

Conclusion

A pSPICE model of a transducer has been used to show how it is possible to deconvolve both linear and non-linear systems. The pSPICE model of the transducer was developed by using electrical and mechanical analogies. To check the method, two examples based on the well known S13 geophone were examined. Particular attention was given to the non-linear case of sliding friction damping. The examples showed that this method can be successful and that it can be applied to deconvolve ancient seismograms from Coulomb damped seismometers.

References:

Cadence Design Systems, Inc. (2005) PSpice® A/D User's Guide, 2005

Geotech instruments LLC. PORTABLE SHORT-PERIOD SEISMOMETER MODEL S-13—Operation and maintenance manual (2000). <http://www.geoinstr.com/pub/manuals/s-13.pdf>. Accessed 13 April 2011

Horowitz P, Hill W (2006) The art of electronics. Cambridge University Press

Romeo G (2012) Whale watching: effects of strong signals on Lippmann style seismometers. J Seismol 16:25–34

Romeo G, abd Braun (2007) Appunti di sismometria. Quaderni di Geofisica 46. http://portale.ingv.it/portale_ingv/produzionescientifica/quaderni-di-geofisica/archivio/quaderni-di-geofisica-2007. Accessed 13 April 2011

Wielandt E (2000) Seismometry. <https://geoazur.oca.eu/IMG/pdf/Seismometry-Cours-WIELANDT.pdf>